Constraints on flux rates and mantle dynamics beneath island arcs from Tonga–Kermadec lava geochemistry

Simon Turner & Chris Hawkesworth

Department of Earth Sciences, The Open University, Milton Keynes MK7 6AA, UK

Subduction processes are central to plate tectonics and to crust–mantle recycling and differentiation. Here we present a study of lavas from the Tonga–Kermadec island arc which places important constraints on the processes and rates involved. The mantle wedge overlying the subducting oceanic plate is dynamically coupled to the descending plate, but may convect more slowly than expected. Fluid and sediment fluxes from the ocean plate enrich the wedge but differ in their location, mechanisms and rates. After partial melting, magma extraction occurs rapidly via channelled flow through the wedge.

A fundamental tenet of modern plate-tectonic theory is the subduction of oceanic plates into the mantle. Subduction induces convective overturn within the mantle wedge[1,2] and may also localize the sheeted downwellings of upper-mantle convection[3]. The surface expressions of subduction are the curved chains of active volcanoes that form island arcs, and the magmatic flux in these volcanoes is an important component of new crustal additions. Conversely, the subduction of oceanic crust and sediments forms the principal mechanism for the recycling of crustal materials into the mantle, contributing to mantle heterogeneity[4]. Thus island arcs play a pivotal role in models for the geochemical evolution of the continental crust and upper mantle, and an understanding of the physical processes and flux rates involved is one of the main goals of the Earth sciences.

Constraints on the dynamics of subduction come from both numerical models and geochemical studies. Recent numerical models[1,2,5] have suggested that convection is induced in the mantle wedge by viscous drag along the upper surface of the subducting oceanic plate and that this controls the thermal structure of the system. The rate of convection is presumably linked to the rate of subduction but the extent of this coupling is poorly constrained, so most models at present assume complete coupling. As we show here, geochemical tracers of specific sediments can be used to constrain the transport time of the subducted sediment signal and thereby provide information on convective overturn in the mantle wedge. It is generally accepted that partial melting and volcanism result from lowering of the peridotite solidus by addition of aqueous fluids from the dehydrating oceanic crust[1,2,5]. However, the rate of fluid flux, its location and whether it occurs vertically[5] or migrates laterally across the mantle wedge[1,2] remain to be determined. Studies of U-series isotope disequilibria have the potential to elucidate the rates of mass transfer. This is because under oxidizing conditions U is mobile in aqueous fluids whereas Th is not[6,7] and the timescales of resultant disequilibria are similar to those of fluid-transfer and melt-generation processes (see, for example, refs 8–13).

Backarc spreading and basalt extraction efficiently depletes the incompatible-element budget of the mantle wedge beneath many island arcs[14]. Consequently, the signatures of contributions from the downgoing slab, particularly ^{238}U-excesses, are best developed in the most depleted arc lavas[15–18]. The Tonga–Kermadec arc is arguably the best place worldwide in which to evaluate mantle wedge dynamics and flux rates because the plate tectonic setting is well documented[19,20] and the very high rates of backarc spreading[20] have made this an exceptionally depleted, end-member arc system[21]. Consistent with this, preliminary U-series isotope data have indicated very large disequilibria in some of the lavas from this arc[16,17]. Here we present selected results from a detailed elemental and isotopic study of Tonga–Kermadec and explore the new constraints these place on the mantle wedge dynamics and flux rates beneath the arc.

Geological background

The intra-oceanic Tonga–Kermadec island arc (Fig. 1) has been formed in response to westward-directed subduction of Jurassic–Cretaceous aged Pacific oceanic lithosphere beneath the Indo-Australian plate since the Oligocene epoch. Splitting of the arc around 3–6 Myr ago initiated active backarc spreading and formation of the Lau basin and Havre trough behind the Tonga–Kermadec ridge[19,20,22–24]. The Tonga and Kermadec portions of the arc are divided at the point of subduction of the Louisville ridge[19] and the present-day arc has a crustal thickness of 12–18 km and lies on volcanic basement[25]. Convergence and backarc spreading rates both increase northwards along the arc (Fig. 1 and ref. 20) and the dip of the Benioff zone is ~28–30° to a depth of ~100 km (the average depth beneath the arc volcanoes) after which it steepens to 55–60° beneath the Kermadecs and 43–45° beneath Tonga[26]. The volcanic products consist of tholeiitic basalts to basaltic andesites with lesser dacites and rhyolites and have phenocryst equilibration temperatures of 1,230–1,120 °C (ref. 25).

Analytical results and implications

We selected 58 samples spanning the length of the arc; we also selected 19 samples of the sediments cored at Deep Sea Drilling Program (DSDP) Site 204 and lavas from the backarc island of Niuafo'ou which lies in the Lau basin some 200 km behind the northern Tongan arc (see Fig. 1). The full data set is presented elsewhere[27]; selected results, pertinent to the arguments below, are given in Table 1.

The geochemical and isotopic data reveal that four components are involved in the petrogenesis of the Tonga–Kermadec lavas. On a ^{208}Pb/^{204}Pb–^{206}Pb/^{204}Pb diagram (Fig. 2a), most of the Tongan lavas overlap the field for the backarc basalts from the Lau basin[24] which are taken as representative of the mantle wedge composition. The

Kermadec lavas extend from this array towards elevated $^{208}Pb/^{204}Pb$. In marked contrast, the lavas from the northernmost Tongan islands of Tafahi and Niuatoputapu are strongly displaced to high $^{206}Pb/^{204}Pb$. The extremely depleted nature of the lavas is exemplified by the concentrations of high-field-strength elements (for example, Ta and Nb) and rare-earth elements (for example, Nd), which are 10 times lower than in typical mid-ocean-ridge basalts (MORBs) and are in fact more comparable with abundances in the MORB source. The large-ion lithophile elements (for example, Ba) are enriched relative to the high-field-strength elements and rare-earth elements (for example, Ba/Ta = 1,465–10,774) although absolute concentrations remain very low. This indicates that the large-ion lithophile elements have been decoupled from the high-field-strength elements and rare-earth elements; this is widely interpreted in terms of a flux of large-ion lithophile elements from the subducting slab into a mantle wedge that was variously depleted in incompatible elements during multi-stage backarc basalt extraction[21,27]. Therefore, one of the surprising results is that Ta and Nb abundances are not lowest in the most-depleted rocks from Tafahi and Niuatoputapu where Ba/Ta = 1,465–2,145.

Table 1 Selected data for Tonga–Kermadec lavas

Island	Mg (wt%)	Ba (p.p.m.)	Th (p.p.m.)	U (p.p.m.)	Ta (p.p.m.)	Nd (p.p.m.)	$^{87}Sr/^{86}Sr$	$^{143}Nd/^{144}Nd$	$^{206}Pb/^{204}Pb$	$^{208}Pb/^{204}Pb$	$(^{230}Th/^{232}Th)$
Tafahi	7.47	33	0.096	0.051	0.02	1.5	0.70388	0.512930	18.978	38.560	1.215
Niuatoputapu	3.31	120	0.399	0.174	0.06	4.3	0.70397	0.512874	19.020	38.720	1.195
Fonualei	1.54	206	0.487	0.472	0.05	7.6	0.70376	0.512992	18.533	38.141	1.652
Late	3.29	165	0.236	0.206	0.03	5.5	0.70369	0.512942	18.518	38.125	1.603
Metis Shoal	5.15	362	0.308	0.230	0.04	5.6	0.70348	0.512980	18.473	37.986	1.821
Kao	5.56	123	0.188	0.140	0.03	6.0	0.70328	0.513068	18.454	37.995	1.401
Tofua	6.16	95	0.132	0.119	0.01	3.0	0.70370	0.513020	18.527	38.098	1.645
Hunga Ha'apai	4.16	119	0.121	0.116	0.03	3.0	0.70371	0.513040	18.516	38.148	1.799
'Ata	6.72	102	0.266	0.136	0.02	4.6	0.70344	0.513087	18.686	38.240	1.335
Raoul	4.82	87	0.235	0.164	0.02	5.7	0.70341	0.513030	18.686	38.371	1.273
Macauley	5.45	119	0.438	0.231	0.02	8.1	0.70343	0.513024	18.675	38.306	1.144
L'Esperance	4.87	121	0.460	0.155	0.03	5.5	0.70394	0.512951	18.729	38.427	0.874
Rumble III	6.47	230	0.416	0.176	0.04	8.8	0.70409	0.513032	18.721	38.538	1.016
Niuafo'ou	7.16	44	0.309	0.095	0.29	12.3	0.70432	0.512834	18.266	38.202	1.026

Methods of analysis: MgO, X-ray fluorescence; Ba, Ta and Nd, inductively coupled plasma mass spectrometry; Th and U, and isotopes of Nd, Pb and Th isotopes, thermal ionization mass spectrometry (see refs 9 and 27 for details).

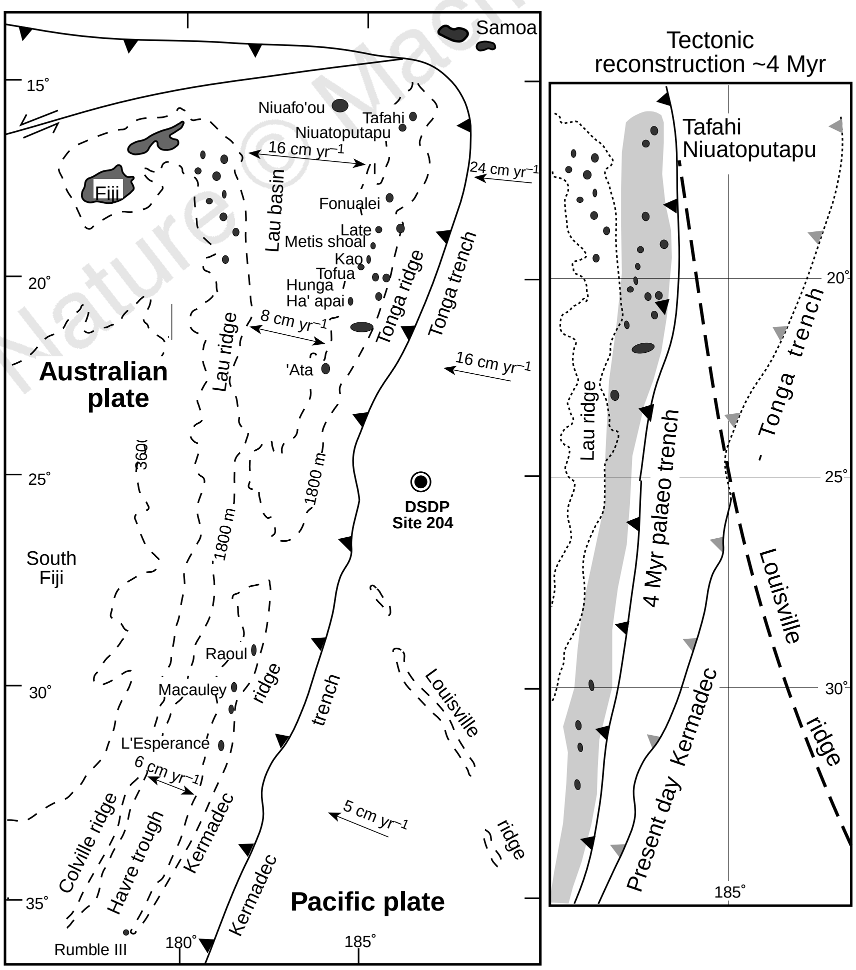

Figure 1 Map of the Tonga–Kermadec island arc system. This figure shows the bathymetry, locations of islands from which samples analysed in this study were taken, and the broad tectonic architecture with estimated plate motions indicated. Convergence and backarc spreading rates both increase northwards along the arc from 50 to 240 mm yr^{-1} and 60 to 160 mm yr^{-1} respectively[20]. DSDP Site 204 from which the subducting sediments have been analysed in detail[27] is also shown (sites 595/596 are ~1,000 km further east). The angle between the Louisville ridge and the arc (which is broadly orthogonal to the motion of the Pacific plate) causes the locus of intersection to migrate southwards with time; the right-hand panel is a tectonic reconstruction[19] showing that the Louisville ridge and its surrounding apron of volcaniclastic sediments would have been being subducted beneath the northern Tongan islands of Tafahi and Niuaptoputapu ~4 Myr ago.

In Fig. 2b most of the lavas form an array in which decreases in $^{143}Nd/^{144}Nd$ are accompanied by constant, or very slightly decreasing, Ta/Nd. Mass-balance calculations[9,10,27–29] have shown that addition of even very small amounts of subducted sediment to the source of the arc lavas will dominate the final Th, Ta-Nb, Zr and rare-earth-element budget of the lavas and consequently dictate their Nd- and Th-isotope signatures[9,10,13,27,28] (isotopes of Sr and Pb reflect a more complex balance between the relative compositions and contributions from the fluid and sediment[9,27,30,31]). Thus, the low Ta/Nd and $^{143}Nd/^{144}Nd$ coupled with elevated $^{208}Pb/^{204}Pb$ are consistent with a sediment contribution to the lavas (see below). But the Tafahi and Niuatoputapu lavas, which were displaced to high $^{206}Pb/^{204}Pb$ in Fig. 2a, show a trend of increasing Ta/Nd with decreasing $^{143}Nd/^{144}Nd$ (Fig. 2b). Such a trend is extremely unusual in arc rocks and these lavas must be influenced by a component which is not seen elsewhere in the arc. Finally, Fig. 2c shows that the lavas form a steep negative array between Ba/Th and $^{206}Pb/^{204}Pb$ which does not fall on any simple mixing line between the Lau basin mantle and subducted sediment; this emphasizes the need for a fluid component with high Ba/Th (refs 9, 13, 28). The implied Pb isotopic signature of this fluid is significantly lower than that of the subducting sediment (Fig. 2c) and so the fluids are inferred to be derived by dehydration of the subducting altered oceanic crust rather than the subducted sediments[9,13,30].

Any model for the Tonga–Kermadec data therefore requires four components—the depleted mantle wedge, separate fluid and sediment contributions[9,10,13,28], and a fourth component characterized by high Ta/Nd and $^{206}Pb/^{204}Pb$ and low $^{143}Nd/^{144}Nd$ seen only in lavas from Tafahi and Niuatoputapu. Our U–Th isotope results are shown in Fig. 3 and include the most extreme ratios yet reported, with up to 50% ^{238}U excesses. The lavas from the backarc island of Niuafo'ou show no evidence for a contribution from the fluid or sediment components identified in the arc lavas (Fig. 2) and lie to the left of the equiline in Fig. 3 with 10–30% ^{230}Th excesses similar to those observed in MORB (see, for example, ref. 32).

Sediment flux

The sediments being subducted beneath the Tonga–Kermadec arc on the downgrowing Pacific plate have been intersected at DSDP Site 204 (Fig. 1) and sites 595/596 located ~1,000 km east of the trench. The total thickness is ~150 m and this is dominantly composed of siliceous ooze and clay throughout sites 595/596 and in the upper 103 m of Site 204. The average composition of this pelagic material is broadly similar to that of average upper crust[29,27,33] and forms an appropriate end-member for the sediment-dominated trend observed in most of the lavas in Fig. 2a, b (that is, towards high $^{208}Pb/^{204}Pb$ and low Ta/Nd, $^{143}Nd/^{144}Nd$). The mixing line between the Lau basin mantle and subducted pelagic sediment in Fig. 2b suggests that the amount added is <1%, implying that most of the subducted sediment is recycled into the upper mantle.

In contrast, the basal 44 m from DSDP Site 204 is dominated by

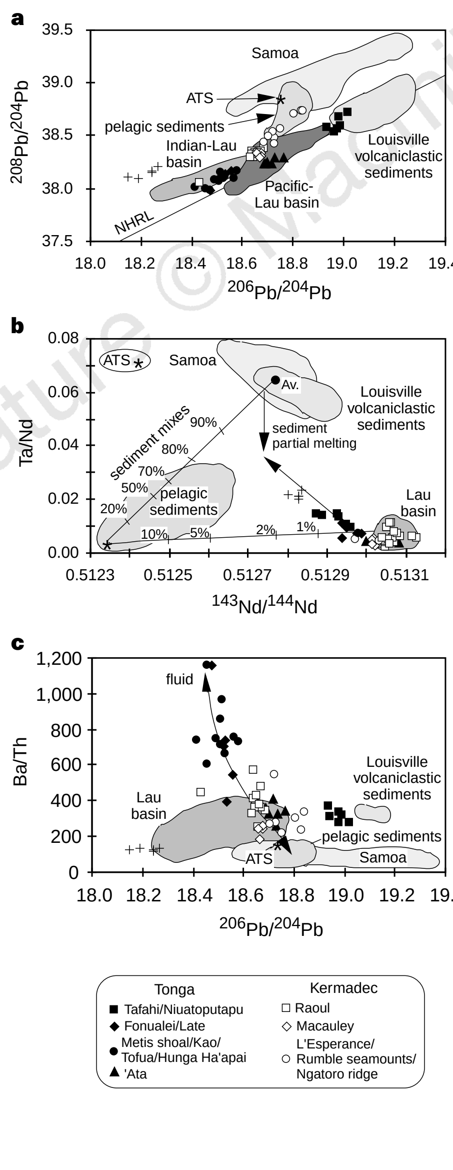

Figure 2 Geochemical and isotopic properties of the Tonga–Kermadec lavas. **a**, $^{208}Pb/^{204}Pb$ versus $^{206}Pb/^{204}Pb$ diagram showing the distinction between the average pelagic sediment (ATS)[33] being subducted beneath the arc and the Louisville volcaniclastic-dominated sediments from the base of DSDP 204 (ref. 27). The Tonga–Kermadec lavas lie on a mixing array between mantle wedge (represented by the basalt array from the Lau basin[24]) and the pelagic sediments, excepting those from Tafahi and Niuatoputapu which are strongly displaced towards the Louisville volcaniclastics but not Samoa (data from refs 50 and 51). NHRL is the northern hemisphere reference line. **b**, Ta/Nd versus $^{143}Nd/^{144}Nd$ diagram, showing that most of the Tonga–Kermadec lavas lie on a mixing line (numbers along the curves indicate the amounts of sediment) between the Lau basin mantle and the average subducted pelagic sediment. In contrast, the Tafahi and Niuatoputapu lavas lie on a different vector displaced to high Ta/Nd and the sediment contribution to these lavas is implied to be a ~10 : 90 mixture of pelagic and Louisville volcaniclastic sediments. In practice, because of the high Pb content of the pelagic sediments, such a mixture would have a $^{206}Pb/^{204}Pb$ ratio of ~18.91 which is too low to explain the Tafahi–Niuatoputapu Pb isotope data (compare **a**). This constraint is relaxed if the sediment mixture was closer to 99% Louisville volcaniclastics. However, such a mixture will have a Ta/Nd ratio which is too high to lie at the end of the Tafahi–Niuatoputapu trend. Thus, it is suggested that the sediment signature was transferred as a partial melt (see also refs 9, 10, 27), such that its Ta/Nd ratio was reduced from ~0.6 to ~0.35 owing to the presence of residual phases like rutile or ilmenite[47] which preferentially held back Ta and Nb relative to the large-ion lithophile elements and rare-earth elements (see, for example, ref. 52). **c**, Ba/Th versus $^{206}Pb/^{204}Pb$ diagram showing a broad negative array that requires a fluid component as well as the mantle wedge and the subducted sediments. We note that the Tafahi and Niuatoputapu rocks are displaced from this trend towards the Louisville volcaniclastics. The crosses are data from the backarc island of Niuafo'ou.

Cretaceous volcaniclastics derived from the nearby Louisville ridge[34] (see Fig. 1). Consistent with analyses of basalts from the Louisville seamount chain itself[35], these have an ocean-island basalt signature characterized by high Ta/Nd and high $^{206}Pb/^{204}Pb$ (ref. 27) providing a unique geochemical tracer which unveils the identity of the fourth component. Mixing arrays form straight lines on Pb–Pb isotope diagrams such as Fig. 2a which shows how a contribution bearing the Louisville signature accounts for the high $^{206}Pb/^{204}Pb$ signal in the Tafahi–Niuatoputapu lavas. A large volcaniclastic sediment apron also surrounds Samoa just to the north of the Tonga arc (see Fig. 1) and may extend as far south as Tafahi and Niuatoputapu[36], and so it might be argued that the high Ta/Nd and $^{206}Pb/^{204}Pb$ in those lavas reflects a contribution from subducted Samoan volcaniclastics. But because the Samoan plume has much higher $^{208}Pb/^{204}Pb$ than the Louisville volcaniclastics, mixing lines drawn between the Lau basin and Samoa will not pass through the Tafahi–Niuatoputapu data (Fig. 2a). Similarly in Fig. 2c, the Tafahi–Niuatoputapu rocks are displaced towards the Louisville volcaniclastics. Thus, it seems clear that the high Ta/Nd and high $^{206}Pb/^{204}Pb$ in the Tafahi–Niuatoputapu rocks are due to the addition of a Louisville component.

It is significant that, in detail, the data in Fig. 2b require that the contribution is a mixture of the pelagic sediments and the Louisville volcaniclastics. Owing to the age and velocity of the subducting oceanic plate, the Louisville seamounts themselves will be too cold to undergo partial melting[37], and so we conclude that it is the sediments themselves (rather than melts or fluids from the seamounts) that are providing the high $^{206}Pb/^{204}Pb$ and Ta/Nd signal. Furthermore, the data require the Ta/Nd ratio to be fractionated in the sediment component (Fig. 2b) and so it appears that the sediment component is added as partial melts that vein the mantle wedge peridotite[27].

The important point is that the Louisville volcaniclastics are spatially restricted to the proximity of the Louisville ridge; they are not observed at DSDP sites 595/596, for example. This is critical to

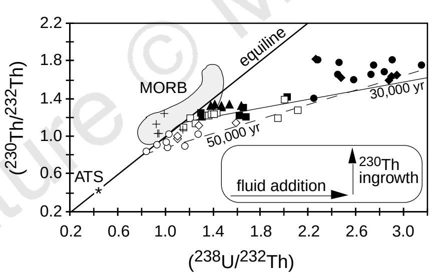

Figure 3 ($^{230}Th/^{232}Th$) versus ($^{238}U/^{232}Th$) (parentheses indicate activity ratios) 'equiline' diagram showing that the Tonga–Kermadec lavas with the largest U-excesses lie on or above a ~50,000-yr reference line (dashed). The simplest interpretation is that this reflects the typical time elapsed between fluid release from the slab and eruption. We attribute age significance to a reference line along the base of the data in preference to a isochron regression though the data because some of the transit times may be longer for some lavas which would result in increases in ^{230}Th and individual samples moving upwards from the reference line. We also note that if the sediment contribution to the Kermadec lavas has lowered their ($^{230}Th/^{232}Th$) intersection with the equiline, then 50,000 yr is probably a maximum estimate of the transfer time and a reference line beneath the Tonga data alone has an age of ~30,000 yr. (The inset illustrates our interpretation of the data.) We note that there is a broad negative correlation between $^{208}Pb^*/^{206}Pb^*$ (radiogenic lead) and ($^{230}Th/^{232}Th$) (ref. 27). Previously, such correlations have been used to argue that the significant, global U/Th variation among arcs is long-lived (that is, several 100 Myr; ref. 17). Within an individual and very depleted arc such as Tonga–Kermadec, such an array is interpreted to represent recent mixing of components (that is, sediment and mangle wedge + fluid) which have themselves had long-lived differences in their U/Th ratios, rather than to imply that the observed variations in U/Th along the arc had existed there for several 100 Myr; ref. 27. Symbols as in Fig. 2, field for MORB from ref. 32.

any evaluation of the time taken for such components to traverse the mantle wedge because the Louisville ridge at present intersects the arc 1,100 km south of Tafahi and Niuatoputapu. The angle between the Louisville ridge and the arc causes the locus of intersection to migrate southwards with time. The present-day convergence rate is 24 cm yr^{-1} but sea-floor spreading rates in the Lau basin have increased in the recent past[38]. If the convergence rate was closer to 8 cm yr^{-1} at the start of backarc spreading 4 Myr ago, then an average convergence rate of ~15 cm yr^{-1} may be more reasonable. Plate reconstructions on the basis of a convergence rate of 15 cm yr^{-1} indicate that the Louisville ridge and its apron of volcaniclastic sediments would have been subducted beneath Tafahi and Niuatoputapu ~4 Myr ago[19] (Fig. 1); this probably represents a maximum age. A striking observation is that the Louisville signature is not observed on the islands south of Niuatoputapu (Fig. 2a, b) and the high $^{143}Nd/^{144}Nd$ ratios (0.51306–0.51308; ref. 22) of 4-Myr-old lavas from the northern Lau ridge, which formed part of the arc before backarc spreading, suggest that the Louisville signature was not present beneath Tafahi and Niuatoputapu 4 Myr ago (unfortunately no Pb isotope or reliable Ta data are available for the Lau ridge lavas). Taken together, and allowing for possible errors in the plate reconstructions, these observations imply that 2–4 Myr elapses between the time of subduction of the sediments and their signature being observed in the arc lavas.

Fluid flux

Experimental data have shown that U (as well as Ba, K, Sr and Pb) is highly mobile in oxidizing aqueous fluids whereas Th behaves as an immobile high-field-strength element[6,7]. Redox conditions will be strongly oxidizing in the altered oceanic crust but reducing in the mantle wedge. Accordingly, the U excesses are taken to reflect the addition of fluids released by dehydration of the subducting oceanic crust[9,10,13,16–18,27,28]. As interaction with the wedge proceeds, the fluids can only become more reducing under which circumstances U will become less mobile and the fractionation of U/Th will diminish. So, the high U/Th results from the initial fluid addition to the wedge and it is those samples with the least sediment contribution (inferred from Nd isotopes[28]) which show the greatest U–Th isotope disequilibria. Such disequilibria are reduced over time by ^{230}Th ingrowth and the data can thus be used to constrain the time elapsed between fluid release from the slab and eruption. The Tonga–Kermadec data indicate that this was of the order of 30,000–50,000 yr (see Fig. 3). Significantly, U–Th isotope data record similar timescales in the Lesser Antilles (~40,000 yr; ref. 9) and in the Marianas (30,000 yr; ref. 10) which provides encouragement for the view that these data reflect some general aspect of the transfer times beneath island arcs.

As shown in Fig. 2c, Ba/Th is fractionated by the fluid and as Ra is likely to behave in an analogous manner to Ba, Ra/Th must also be fractionated by the fluid. However, ^{226}Ra will return to secular equilibrium with ^{230}Th within 7,500 yr of Ra/Th fractionation and well within the inferred time period (30,000–50,000 yr) between fluid release and eruption. Nevertheless, large ^{226}Ra excesses have been reported in several of the same samples analysed for U–Th from Tonga–Kermadec (($^{226}Ra/^{230}Th$) = 1.5–3.0; ref. 16), the Lesser Antilles (($^{226}Ra/^{230}Th$) = 1.2–2.2; ref. 11, 16) and the Marianas (($^{226}Ra/^{230}Th$) = 2.6–3.1; ref. 16). Here the parentheses indicate activity ratios. This would not be expected given the ages inferred for the U–Th data, suggesting that the $^{238}U–^{230}Th$ and $^{226}Ra–^{230}Th$ disequilibria are decoupled (see also ref. 9). In other words, any Ra/Th fractionation produced during fluid release returns to secular equilibrium and the observed $^{226}Ra/^{230}Th$ disequilibria is developed subsequently.

Partial melting and magma extraction

The decoupling between the $^{238}U–^{230}Th$ and $^{226}Ra–^{230}Th$ disequilibria can be integrated into a model for partial melting and magma extraction. Ba (and by analogy Ra) partitions more strongly into plagioclase than Th (ref. 39) and so it might be argued that the ^{226}Ra excesses result from plagioclase accumulation. However, the Tonga–Kermadec major-element data indicate that plagioclase is a fractionating phase and therefore the ^{226}Ra excesses are unlikely to have developed in crustal magma chambers. By analogy with MORB, we suggest that the ^{226}Ra excesses are produced during partial melting and/or magma ascent[8,12,40]. In current melting models for mid-ocean ridges, Ra is not sensitive to the depth of melting and we infer that the ^{226}Ra excesses in arc lavas indicate melt extraction and ascent on timescales no more than 1–2 half lives of ^{226}Ra (that is, 1,600–3,200 yr) which requires channelled flow through the mantle wedge and ascent rates of $\sim$35–70 m yr^{-1}. Similar magma ascent rates have been proposed to occur beneath mid-ocean ridges[8] and there is as yet little reason to suppose that they should be any slower beneath island arcs. In fact, recent numerical modelling suggests that the mantle wedge is likely to be under tension directly beneath the arc volcanoes[41], and high volatile contents would result in low magma viscosities, both of which would promote rapid magma ascent.

Implications for physical models

As illustrated in Fig. 4, our data provide important constraints for physical models of the Tonga–Kermadec island arc and may be applicable to arcs in general.

(1) Recycling of the sediment component is slow; it takes 2–4 Myr after subduction before the Louisville volcaniclastics signature is observed in the arc lavas. Yet the rate of subduction beneath Tonga is 150–240 mm yr^{-1} and so sediments would arrive at the source region beneath the arc volcanoes in <1 Myr if they were transported on the subducting plate. In 2–4 Myr they would have passed several 100 km beyond the arc volcanoes, and yet there is no evidence for a sediment signature in lavas form the backarc island of Niuafo'ou as would be expected if the sediment component was being brought into the arc melt generation zone via convection from the backarc. It might be suggested that the sediments travel on the descending plate to a point beneath the arc volcanoes where they undergo partial melting and that it subsequently takes 2–4 Myr for these melts to migrate upwards to the site of magma generation. However, partial melts of sediments are highly viscous and would freeze in the mantle wedge[42] after which they would be rapidly swept away by the convection in the wedge. The rate of convection in the mantle wedge is generally poorly constrained, but the contrast in velocities of the overlying and downgoing plates clearly demands that there is some decoupling between these plate motions and the mantle wedge.

In our preferred model, partial melts of the sediment are added to the overlying mantle wedge at a relatively shallow level, and the wedge is only partially coupled to the descending slab. As a result, convection and down-dip movement are much slower than the rate of slab descent and this enriched mantle only reaches the melt-generation zone after 2–4 Myr. Depending on the exact point of addition, this constrains the down-dip component of induced convection in the mantle wedge to be 20–40 mm yr^{-1}. We note that this is a maximum range assuming that the sediment signal is imparted to the mantle wedge at shallow levels during subduction (see below), but it is significant that this is similar to the half-spreading rates in the Lau basin. In other words, the mantle convection rate seems to be more closely linked to the rate of motion of the overlying plate than to that of the downgoing plate against which there must therefore be a major component of shear-slip.

(2) In contrast, recycling of the fluid component is relatively fast; the U–Th data indicate only 30,000–50,000 yr has elapsed since fluid release from the slab, and clearly this must have occurred after addition of the sediment (see also ref. 10). Recent experimental data[43] suggest that subducted oceanic crust undergoes pressure-dependent amphibolite to eclogite dehydration reactions at around 70–80 km depth. In some models the resultant fluid flux occurs vertically into the wedge and the amphibole peridotite formed then migrates downwards with convection in the wedge until it crosses its solidus ($\sim$1,000 °C; refs 44, 45) and undergoes partial melting[5]. Alternatively, it has been suggested that the fluid migrates horizontally across the mantle wedge by a combination of vertical rise as a fluid and horizontal translation whilst being dragged down in the wedge in the form of amphibole until it reaches the amphibole peridotite solidus[1,2]. The latter model is consistent with the lack of evidence from the rare-earth elements and U–Th disequilibria that melting occurred in the presence of residual garnet. If the melt generation zone lies at 70–80 km depth, then, assuming that magma

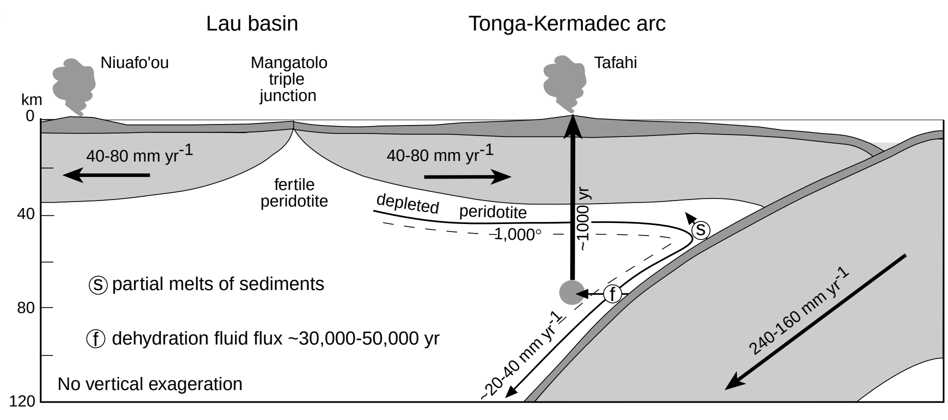

Figure 4 Scaled east–west cross section across the Tonga arc through Tafahi illustrating the inferred mantle wedge dynamics and flux rates beneath the Tonga–Kermadec island arc. The mantle wedge convects at a rate similar to that of the overlying plate and is largely decoupled from the downgoing plate. This produces significant shear-heating along its upper surface at shallow levels which, combined with advection of hot wedge material from the Lau basin, results in partial melting of the subducted sediments which enrich the depleted wedge peridotite at point S. This material is carried down with convection in the wedge for 2–4 Myr until point f where amphibolite in the subducted oceanic crust dehydrates, releasing aqueous fluids. These fluids traverse the wedge[1,2] until the amphibole peridotite solidus (1,000 °C isotherm[44,45]) is reached and partial melting of sediment enriched peridotite occurs. Rapid magma ascent to the surface then occurs via channelled flow. Neither the sediment or fluid components reach the source region for the backarc volcano of Niuafo'ou. We note that the inferred transport time of ~4 Myr for the sediment component would predict that the majority of any ^{10}Be signal from the subducted sediments would have decayed away in this time. Unfortunately, there are as yet no Be isotope data from Tonga–Kermadec to test this. Moreover, because of the condensed nature of the subducting sediment column in the Tonga–Kermadec arc, all of the ^{10}Be may be concentrated in the upper 10 cm and vulnerable to mechanical loss during subduction (see refs 13 and 27 for further discussion of the ^{10}Be signal in arc lavas).

ascent is more or less vertical, it must lie 20–30 km out from the slab such that the arc volcanoes lie ~100 km above the slab. But given the inferred rate of convection in the wedge, the angle of subduction and the 30,000–50,000 yr time constraints for fluid transport, the horizontal component of translation in the wedge is limited to ~1–3 km, suggesting that some other process, such as hydraulic fracture[46], is required to allow fluids to be transported more efficiently through the mantle wedge[13].

(3) The data reported here seem to require a thermal structure within the mantle wedge that is considerably hotter than suggested by recent thermal models[1,2] (this conclusion does depend, however, on the details of the models). Nevertheless, the evidence for partial melting of the subducted sediments (see also refs 9, 10) and the phenocryst equilibration temperatures of the lavas (1,120–1,230 °C) may support the existence of a hotter thermal structure. In numerical models the thermal structure of the wedge is least well defined near the slab–wedge interface[2], and at present there are few experimental studies of partial melting of hydrated sediments under pressure–temperature conditions appropriate to the sub-arc environment[47]. However, sediment melting probably requires temperatures of 650–700 °C. The decoupling required by the relative plate motions and the transfer time of the Louisville component suggest that significant shear occurs against the downgoing plate and, although the effects of shear-heating are poorly constrained, this may increase temperatures by as much as 200 °C at shallow levels[48]. Moreover, the presence of 1.4–2.0 Myr boninites dredged between Tafahi and the trench[49] provides evidence for high temperatures in the wedge close to the trench at that time. Irrespective of the model assumed, the limited time for fluid transport following dehydration of the oceanic crust at 70–80 km depth may even require that the position of the 1,000 °C isotherm and zone of melt generation lies within a few kilometres of the slab–wedge interface between 70 and 100 km depth.

(4) The sediment and fluid signatures are not observed in lavas from the backarc island of Niuafo'ou. This places a maximum limit on the lateral extent to which the subduction signature penetrates into the mantle wedge (<200 km). The Niuafo'ou rocks preserve ^{230}Th excesses similar to MORBs (Fig. 3), consistent with partial melting in the presence of residual garnet and at deeper levels than beneath the arc volcanoes.

(5) Reported ^{226}Ra disequilibria[16] suggest that the U–Th and Ra–Th systematics are decoupled; the simplest explanation is that the observed ^{226}Ra excesses developed during partial melting and magma ascent[8,40] rather than during fluid release for the subducting slab. Thus the magmas, once formed, ascend rapidly (~1,600–3,200 yr) via channelled flow through the mantle wedge to be erupted along the overlying chain of arc volcanoes. □

Received 11 December 1996; accepted 29 July 1997.

1. Davies, J. H. & Bickle, M. J. A physical model for the volume and composition of melt produced by hydrous fluxing above subduction zones. *Phil. Trans. R. Soc. Lond.* **335,** 355–364 (1991).
2. Davies, J. H. & Stevenson, D. J. Physical model of source region of subduction zone volcanics. *J. Geophys. Res.* **97,** 2037–2070 (1992).
3. Bercovici, D., Schubert, G. & Glatzmaier, G. A. Three-dimensional spherical models of convection in the Earth's mantle. *Science* **244,** 950–955 (1989).
4. Hofmann, A. W. Mantle geochemistry: the message for oceanic volcanism. *Nature* **385,** 219–229 (1997).
5. Tatsumi, Y. Migration of fluid phases and genesis of basalt magmas in subduciton zones. *J. Geophys. Res.* **94,** 4697–4707 (1989).
6. Brenan, J. M., Shaw, H. F., Ryerson, F. J. & Phinney, D. L. Mineral-aqueous fluid partitioning of trace elements at 900 °C and 2.0 GPa: constraints on the trace element chemistry of mantle and deep crustal fluids. *Geochim. Cosmochim. Acta* **59,** 3331–33350 (1995).
7. Keppler, H. Constraints from partitioning experiments on the composition of subduction-zone fluids. *Nature* **380,** 237–240 (1996).
8. Richardson, C. & McKenzie, D. Radioactive disequilibria from 2D models of melt generation by plumes and ridges. *Earth Planet. Sci. Lett.* **128,** 425–437 (1994).
9. Turner, S. *et al.* U-series isotopes and destructive plate margin magma genesis in the Lesser Antilles. *Earth Planet. Sci. Lett.* **142,** 191–207 (1996).
10. Elliott, T., Plank, T., Zindler, A., White, W. & Bourdon, B. Element transport from slab to volcanic front at the Mariana arc. *J. Geophys. Res.* **102,** 14991–15019 (1997).
11. Chabaux, F. & Allègre, C. J. ^{238}U-^{230}Th-^{226}Ra disequilibria in volcanics: a new insight into melting conditions. *Earth Planet. Sci. Lett.* **126,** 61–74 (1994).
12. Beattie, P. Uranium-thorium disequilibria and partitioning on melting of garnet peridotite. *Nature* **363,** 63–65 (1993).
13. Hawkesworth, C. J., Turner, S. P., McDermott, F., Peate, D. W. & van Calsteren, P. U-Th isotopes in arc magmas: implications for element transfer from the subducted crust. *Science* **276,** 551–555 (1997).
14. Woodhead, J., Eggins, S. & Gamble, J. High field strength and transition element systematics in island arc and back-arc basin basalts: evidence for multi-phase melt extraction and a depleted mantle wedge. *Earth Planet. Sci. Lett.* **114,** 491–504 (1993).
15. Hawkesworth, C. J., Gallagher, K., Hergt, J. M. & McDermott, F. Mantle and slab contributions in arc magmas. *Annu. Rev. Earth Planet. Sci.* **21,** 175–204 (1993).
16. Gill, J. B. & Williams, R. W. Th isotope and U-series studies of subduction-related volcanic rocks. *Geochim. Cosmochim. Acta* **54,** 1427–1442 (1990).
17. McDermott, F. & Hawkesworth, C. J. Th, Pb and Sr isotope variations in young island arc volcanics and oceanic sediments. *Earth Planet. Sci. Lett.* **104,** 1–15 (1991).
18. Condomines, M. & Sigmarsson, O. Why are so many arc magmas close to ^{238}U-^{230}Th radioactive equilibrium? *Geochim. Cosmochim. Acta* **57,** 4491–4497 (1993).
19. Dupont, J. & Herzer, R. H. in *Geology and Offshore Resources of Pacific Island arcs—Tonga Region* (eds Scholl, D. W. & Vallier, T. L.) 323–332 (Circum-Pacific Council for Energy and Mineral Resources, Houston, 1985).
20. Bevis, M. *et al.* Geodetic observations of very rapid convergence and back-arc extension at the Tonga arc. *Nature* **374,** 249–251 (1995).
21. Ewart, A. & Hawkesworth, C. J. The Pleistocene-Recent Tonga-Kermadec arc lavas: Interpretation of new isotopic and rare earth data in terms of a depleted mantle source model. *J. Petrol.* **28,** 495–530 (1987).
22. Cole, J. W., Graham, I. J. & Gibson, I. L. Magmatic evolution of Late Cenozoic volcanic rocks of the Lau Ridge, Fiji. *Contrib. Mineral. Petrol.* **104,** 540–554 (1990).
23. Ewart, A., Bryan, W. B., Chappell, B. W. & Rudnick, R. L. Regional Geochemistry of the Lau-Tonga arc and backarc systems. *Proc. ODP Sci. Res.* **135,** 385–425 (1994).
24. Hergt, J. M. & Hawkesworth, C. J. Pb-, Sr-, and Nd-isotopic evolution ofthe Lau Basin: implications for mantle dynamics during backarc opening. *Proc. ODP Sci. Res.* **135,** 505–517 (1994).
25. Ewart, A., Brothers, R. N. & Mateen, A. An outline of the geology and geochemistry, and the possible petrogenetic evolution of the volcanic rocks of the Tonga-Kermadec-New Zealand island arc. *J. Volcanol. Geotherm. Res.* **2,** 205–250 (1977).
26. Isacks, B. L. & Barazangi, M. in *Island Arcs, Deep Sea Trenches, and Back-Arc Basins* (eds Talwani, M. & Pitman, W. C.) 99–114 (Am. Geophys. Un., Washington DC, 1977).
27. Turner, S. *et al.* ^{238}U-^{230}Th disequilibria, magma petrogenesis and flux rates beneath the depleted Tonga-Kermadec island arc. *Geochim. Cosmochim. Acta* (in the press).
28. Hawkesworth, C., Turner, S., Peate, D., McDermott, F. & van Calsteren, P. Elemental U and Th variations in island arc rocks: implications for U-series isotopes. *Chem. Geol.* **139,** 207–221 (1997).
29. Plank, T. & Langmuir, C. H. Tracing trace elements from sediment input to volcanic output at subduction zones. *Nature* **362,** 739–743 (1993).
30. Miller, D. M., Goldstein, S. L. & Langmuir, C. H. Cerium/lead and lead isotope ratios in arc magmas and the enrichment of lead in the continents. *Nature* **368,** 514–520 (1994).
31. Brenan, J. M., Shaw, H. F. & Ryerson, J. Experimental evidence for the origin of lead enrichment in convergent-margin magmas. *Nature* **378,** 54–56 (1995).
32. Bourdon, B., Zindler, A., Elliott, T. & Langmuir, C. H. Constraints on mantle melting at mid-ocean ridges from global ^{238}U-^{230}Th disequilibrium data. *Nature* **384,** 231–235 (1996).
33. Plank, T. & Langmuir, C. H. The geochemical composition of subducting sediment and its consequences for the crust and mantle. *Chem. Geol.* (in the press).
34. Burns, R. E. *et al.* Site 204. *Init. Rep. DSDP* **21,** 33–56 (1973).
35. Cheng, Q. *et al.* Isotopic evidence for a hotspot origin of the Louisville seamount chain. *Am. Geophys. Un. Monogr., Washington DC* **43,** 283–296 (1987).
36. Lonsdale, P. Sedimentation and tectonic modification of Samoan archipelagic apron. *Am. Assoc. Petrol. Geol. Bull.* **59,** 780–798 (1975).
37. Peacock, S. M., Rushmer, T. & Thompson, A. B. Partial melting of subducting oceanic crust. *Earth Planet. Sci. Lett.* **121,** 227–244 (1994).
38. Taylor, B., Zellmer, K., Martinez, F. & Goodliffe, A. Sea-floor spreading in the Lau back-arc basin. *Earth Planet. Sci. Lett.* **144,** 35–40 (1996).
39. Dunn, T. & Sen, C. Mineral/matrix partition coefficients for orthopyroxene, plagioclase, and olivine in basaltic to andesitic systems: a combined analytical and experimental study. *Geochim. Cosmochim. Acta* **58,** 717–733 (1994).
40. Spiegelman, M. & Elliott, T. Consequences of melt transport for uranium series disequilibrium in young lavas. *Earth Planet. Sci. Lett.* **118,** 1–20 (1993).
41. Furukawa, Y. Magmatic processes under arcs and formation of the volcanic front. *J. Geophys. Res.* **98,** 8309–8319 (1993).
42. McKenzie, D. The extraction of magma from the crust and mantle. *Earth Planet. Sci. Lett.* **74,** 81–91 (1985).
43. Liu, J., Bohlen, S. R. & Ernst, W. G. Stability of hydrous phases in subducting oceanic crust. *Earth Planet. Sci. Lett.* **143,** 161–171 (1996).
44. Green, D. H. Experimental melting studies on a model upper mantle composition at high pressure under water-saturated and water-undersaturated conditions. *Tectonophysics* **17,** 285–297 (1973).
45. Wyllie, P. J. Magmas and volatiles components. *Am. Mineral.* **64,** 469–500 (1979).
46. Davies, J. H. & Rowland, A. Importance of temperature dependent viscosity and hydraulic fracture on physical models of subduction zone magmatism. *Geol. Soc. Aust. Abstr.* **45,** 17–20 (1997).
47. Nichols, G. T., Wyllie, P. J. & Stern, C. R. Subduction zone melting of pelagic sediments constrained by melting experiments. *Nature* **371,** 785–788 (1994).
48. Molnar, P. & England, P. Temperatures in zones of steady-state underthrusting of young oceanic lithosphere. *Earth Planet. Sci. Lett.* **131,** 57–70 (1995).
49. Danyushevsky, L. V., Sobolev, A. V. & Falloon, T. J. North Tongan high-Ca boninite petrogenesis: the role of Samoan plume and subduction zone-transform fault transition. *J. Geodyn.* **20,** 219–241 (1995).
50. Palacz, Z. A. & Saunders, A. Coupled trace element and isotope enrichment in the Cook-Austral-Samoa islands, southwest Pacific. *Earth Planet. Sci. Lett.* **79,** 270–280 (1986).
51. Wright, E. & White, W. M. The origin of Samoa: new evidence from Sr, Nd, and Pb isotopes. *Earth Planet. Sci. Lett.* **81,** 151–162 (1986).
52. Jenner, G. A. *et al.* Determination of partition coefficients from trace elements in high pressure-temperature experimental run products by laser ablation microprobe-inductively coupled plasma-mass spectrometry (LAM-ICP-MS). *Geochim. Cosmochim. Acta* **58,** 5099–5103 (1994).

Acknowledgements. We thank H. Davies, T. Plank, D. Peate, N. Rogers, J. Hergt, I. Smith, T. Worthington, A. Cohen and P. van Calsteren for discussions about island arc magma petrogenesis and U-series disequilibria generally; J. Bartlett and N. Rogers for providing analytical assistance; I. Smith, T. Worthington, J. Pearce, S. Acland, T. Vallier and J. Gill for providing us with samples; T. Plank for allowing us to refer to her work in press; and T. Plank for reviews of the manuscript. This work was supported in part by the NERC, and S.T. was supported by a Royal Society University Research Fellowship.

Correspondence and requests for materials should be addressed to S.T. (e-mail: s.p.turner@open.ac.uk).